Science

AAAS

Crystal Structure of a Mammalian
Voltage-Dependent Shaker Family K+ Channel
Stephen B. Long, *et al.*
Science **309**, 897 (2005);
DOI: 10.1126/science.1116269

Crystal Structure of a Mammalian Voltage-Dependent *Shaker* Family K$^+$ Channel

Stephen B. Long, Ernest B. Campbell, Roderick MacKinnon*

Voltage-dependent potassium ion (K$^+$) channels (Kv channels) conduct K$^+$ ions across the cell membrane in response to changes in the membrane voltage, thereby regulating neuronal excitability by modulating the shape and frequency of action potentials. Here we report the crystal structure, at a resolution of 2.9 angstroms, of a mammalian Kv channel, Kv1.2, which is a member of the *Shaker* K$^+$ channel family. This structure is in complex with an oxido-reductase β subunit of the kind that can regulate mammalian Kv channels in their native cell environment. The activation gate of the pore is open. Large side portals communicate between the pore and the cytoplasm. Electrostatic properties of the side portals and positions of the T1 domain and β subunit are consistent with electrophysiological studies of inactivation gating and with the possibility of K$^+$ channel regulation by the β subunit.

Voltage-dependent K$^+$ (Kv) channels are members of the voltage-dependent cation channel family, which includes the voltage-dependent K$^+$, Na$^+$, and Ca^{2+} channels (*1*). These channels are present in all the major kingdoms of life. In eukaryotic cells, they work in concert with other ion channels to produce and modulate the electrical activity of the cell. This electrical activity is important for many processes in electrically excitable cells such as neurons and muscle, as well as in nonexcitable cells (*1*). In the quintessential excitable cell, the neuron, Kv channels return the membrane voltage to its negative resting value after an action potential, modulate the shape of action potentials, and set the action potential firing rate (*1*).

Most of our knowledge of Kv channel function comes from studies of the *Shaker* K$^+$ channel from *Drosophila melanogaster* and its family members from mammalian cells (*2*). *Shaker* family channels have been extensively studied with electrophysiology, because they can easily be expressed in *Xenopus laevis* oocytes and in other cells. In contrast, nearly all of our knowledge of K$^+$ channel structure is based on studies of prokaryotic K$^+$ channels, because they are more easily expressed at high levels in *Escherichia coli*. Such studies have taught us much about their pores, selectivity filters, and gates (*3*).

Eukaryotic Kv channels in many respects are very similar to their prokaryotic counter-

Howard Hughes Medical Institute, Laboratory of Molecular Neurobiology and Biophysics, Rockefeller University, 1230 York Avenue, New York, NY 10021, USA.

*To whom correspondence should be addressed. E-mail: mackinn@rockefeller.edu

parts. The selectivity filter sequence is so conserved that we expect its structure to be essentially the same in all K$^+$ channels. The pore's "inverted teepee" arrangement of inner helices, which holds the selectivity filter in its wider half near the extracellular surface, is also expected to be a conserved feature (*4*). However, beyond their conserved pore and certain domains that regulate the opening of the pore's gate, eukaryotic Kv channels have certain unique features. For example, in the S6 inner helix (on the intracellular side of the selectivity filter), a highly conserved triplet sequence, Pro-X-Pro (where X is any amino acid), is present in *Shaker* family Kv channels but not in prokaryotic Kv channels. Mutations show that this sequence is very important for gating, but the reason why has yet to be determined (*5*, *6*). There has been speculation that this region of the pore (the inner pore), which is lined by the S6 inner helices, is different in *Shaker* Kv channels (*5*, *7*) than in prokaryotes.

Shaker family Kv channels have an adaptation that, as far as we know, does not exist in prokaryotic Kv channels, and apparently allows them to carry out tasks that are unique to eukaryotic cells. Preceding the first membrane-spanning helix, S1, the N terminus forms a T1 domain inside the cell (*8–11*). Four T1 domains, one from each of the four *Shaker* Kv channel subunits, come together to form a tetrameric assembly at the intracellular membrane surface. This domain is located directly over the pore entryway to the cytoplasm, which means that the transmembrane pore must communicate with the cytoplasm through side portals in order to allow K$^+$ ions to flow freely between the cell and the transmembrane pore (*12–14*). These portals not only permit

K$^+$ ions, but they also must be large enough to allow the entry of a polypeptide chain from the channel's N terminus, which functions as an inactivation gate in some *Shaker* family Kv channels (*15*, *16*).

The T1 domain in eukaryotic Kv channels is a docking platform for the β subunit (*12*, *17*, *18*). The β subunit forms a tetramer of proteins related to aldo-keto reductase enzymes, which are oxido-reductases dependent on NADPH (the reduced form of nicotinamide adenine dinucleotide phosphate), with α-β barrel structures (*19–24*). Crystal structures of a β subunit tetramer and of a β-T1 domain complex showed that the enzyme's active site contains an NADP$^+$ cofactor and catalytic residues for hydride transfer (*12*, *24*). The β subunit active site is mysterious because its function is still unknown. Is it an enzyme that can be regulated by a Kv channel or does it serve as a sensor for the Kv channel, allowing the redox state of a cell to influence electrical activity at the membrane? Nearly all *Shaker* family Kv channels in the mammalian nervous system are associated with these oxido-reductase β subunits (*25*).

Experimental evidence suggests that voltage-dependent gating is fundamentally similar in prokaryotic and eukaryotic Kv channels and that their voltage sensors are structurally similar (*26–29*). But structural studies with *Shaker* family Kv channels have the potential to be more informative. The structures of the prokaryotic Kv channel KvAP suggest that an intact lipid membrane is required to keep the voltage sensors correctly oriented with respect to the pore (*30*) [see also Protein Data Bank (PDB) ID 2A0L]. Because the membrane is removed during isolation of the channel, this requirement has so far obscured all attempts to deduce the structural basis for electro-mechanical coupling between the voltage sensor and the pore. The voltage sensor in *Shaker* family Kv channels is constrained by its attachment to a cytoplasmic T1 domain, and therefore may maintain its tenuous but important connections to the pore.

Structure of the Kv1.2–β subunit complex. The Kv1.2 K$^+$ channel from rat brain (*31*) was coexpressed with the β2 K$^+$ channel β subunit from rat brain (*32*) in the yeast *Pichia pastoris* as described in (*33*) with modifications (*34*). The protein was purified and crystallized (*34*). Throughout purification and crystallization, it was necessary to keep the protein in a mixture of detergent (*n*-dodecyl-β-D-maltopyranoside or *n*-decyl-β-D-maltopyranoside) and lipids {1-palmitoyl-2-oleoyl-*sn*-glycero-3-phosphocholine, 1-palmitoyl-2-oleoyl-*sn*-glycero-3-phosphoethanolamine, and 1-palmitoyl-2-oleoyl-*sn*-glycero-3-[phospho-*rac*-(1-glycerol)]}; to maintain a strongly re-
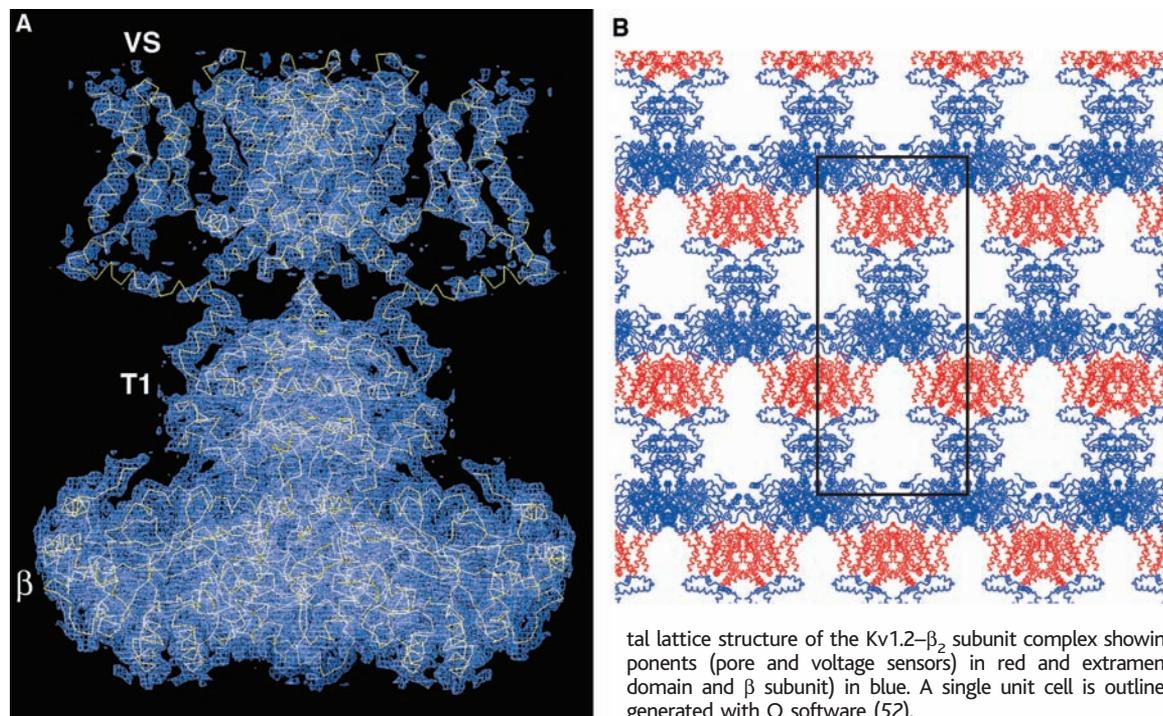
Fig. 1. Electron density and crystal lattice of the Kv1.2–β2 subunit complex. (**A**) The electron density map (blue mesh) was calculated at 2.9 Å resolution using $2F_o - F_c$ (where F_o is the observed structure factor and F_c is the calculated structure factor) amplitudes and phases from a model without voltage sensors and T1-S1 linkers. It is contoured at 0.8σ. A C_α trace of the final model is shown (yellow). The integral membrane pore and voltage sensors (VS) are on top, the T1 domain in the middle, and the β subunit on the bottom. (**B**) Crystal lattice structure of the Kv1.2–β₂ subunit complex showing integral membrane components (pore and voltage sensors) in red and extramembranous components (T1 domain and β subunit) in blue. A single unit cell is outlined in black. The figure was generated with O software (52).

ducing environment with dithiothreitol (DTT) and tri(2-carboxyethyl)phosphine hydrochloride (TCEP); and to keep the protein in an oxygen-depleted atmosphere. Crystals in space group *I*4, grown by vapor diffusion and frozen in liquid nitrogen, diffracted x-rays to 2.9 Å Bragg spacings at the synchrotron (Table 1). Phases were determined by molecular replacement by using the crystal structure of the T1 domain–β2 complex (PDB ID 1EXB) (*12*). Electron density for the transmembrane pore and voltage sensors visible in initial maps (Fig. 1A) allowed us to construct a model through cycles of model building, refinement, and map calculation. Figure 1B shows the structure of the crystal lattice, which consists of layers of membrane-spanning regions (pore and voltage sensors in red) alternating with extramembranous regions (T1 domains and β subunits in blue). This arrangement closely mimics a native membrane organization with coplanar arrays of transmembrane elements pointed in the same direction. The quality of electron density varies over the molecule, with T1 and β stronger (mean *B* factor = 59 Å²), and the pore (mean *B* factor = 159 Å²) and voltage sensor (mean *B* factor = 162 Å²) weaker. This variation is understandable in terms of lattice contacts within the crystal and in terms of the function of different components of the channel. The T1 domains and β subunits are rigid structures and well packed in the β subunit layer. The pore is somewhat more flexible in the inner leaflet of the membrane, and the voltage sensors are highly mobile domains that are suspended, making few contacts with neighboring protein molecules. The β subunit, T1 domain, pore (S5, pore helix,

filter, and S6), and the S4-S5 linker helix were built as essentially complete models with most side chains included. Four main transmembrane segments of the voltage sensor (S1 to S4) were built without connecting the loops S1-S2, S2-S3, and S3-S4. Prior knowledge of the KvAP structure was helpful in building the voltage sensor, because electron density for side chains was weakest in this region of the channel. The linker connecting the T1 domain to S1 was built as two poly-glycine helices.

The complete Kv1.2 channel–β2 subunit complex has fourfold symmetry corresponding to the tetrad axis of the *I*4 unit cell (Fig. 2, A to C). The dimensions of the tetramer are approximately 135 Å by 95 Å by 95 Å. The pore and four voltage sensors are ~30 Å in length across the membrane, corresponding to the known thickness of the hydrophobic core of the membrane. The T1 domain and β subunit are each ~40 Å in length along the fourfold axis. The T1 domain is offset (parallel to the fourfold axis) from the intracellular pore opening by ~15 to 20 Å. The α-helical T1-S1 linker appears to function as a spacer to maintain separation between the transmembrane pore and intracellular regions of the channel.

Table 1. Data collection, phasing, and refinement statistics. *I*, intensity; *F*, amplitude; ASU, asymmetric unit; NSLS, National Synchrotron Light Source.
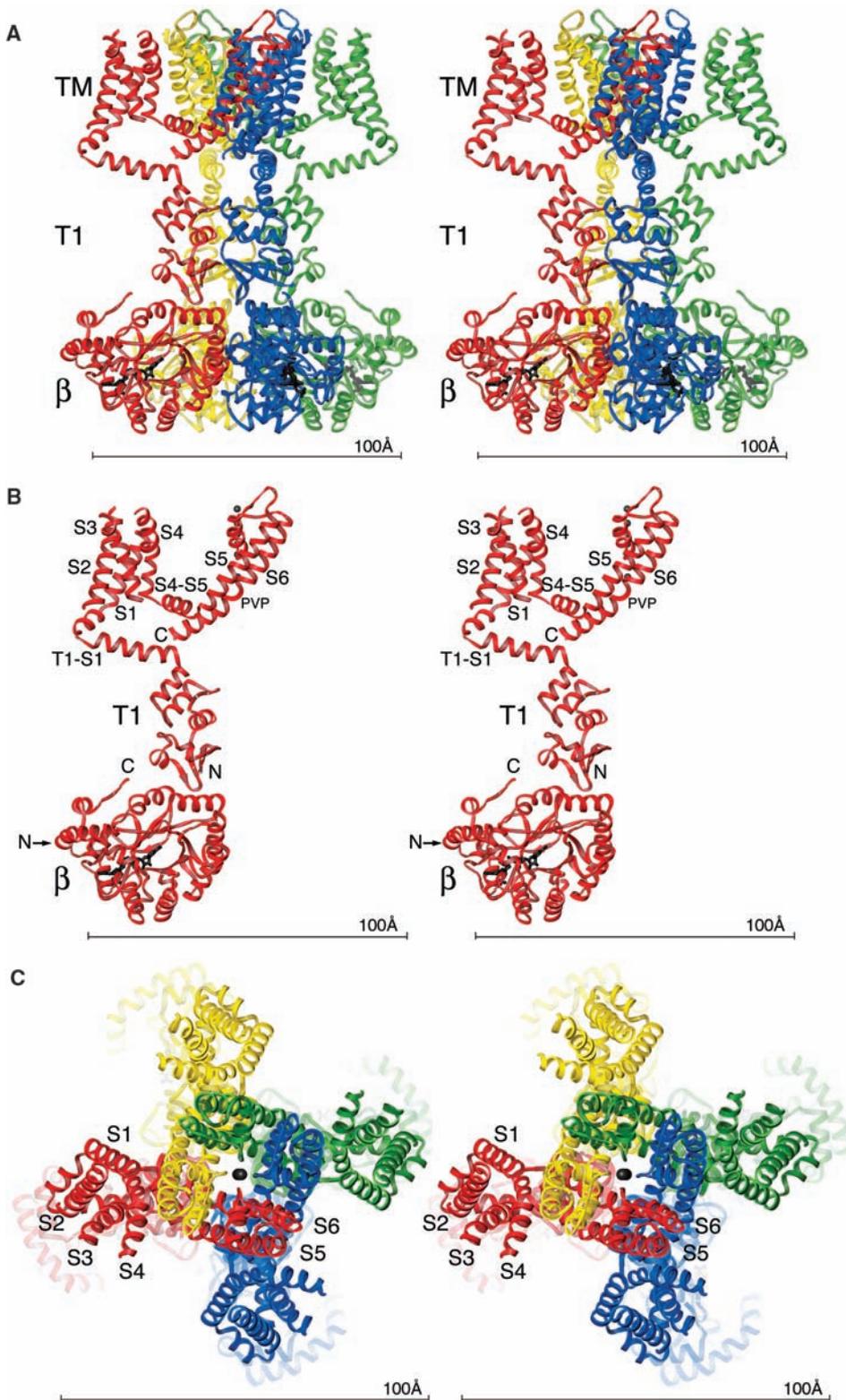
Data collection ($I \geq -3\sigma_I$):	
Space group	*I*4
Cell parameters (Å)	113.6, 113.6, 260.5
Source	NSLS X-25
Resolution (Å)	30.0 to 2.9
Wavelength (Å)	1.1
No. of reflections (total)	105,594
No. of reflections (unique)	36,056
Completeness (%)	99.0 (99.9)*
R_{sym} (%)†	7.2 (47.7)
I/σ	10.8 (2.1)

Refinement (30 to 2.9 Å, $F \geq 0\sigma_F$):	
No. of reflections (work + free) 33,343	No. of atoms 4,997
No. of molecules/ASU	1
R_{work}/R_{free} (%)‡	22.2/25.2
Bond length/angle§	0.01 Å/1.3°
Ramachandran	99.8% (allowed region)/0.02% (disallowed region)

*The parentheses indicate the outer resolution shell (3.0 to 2.9 Å).   †$R_{sym} = \Sigma|I_i - \langle I_i \rangle|/\Sigma I_i$, where $\langle I_i \rangle$ is the average intensity of symmetry-equivalent reflections.   ‡R factor $= \Sigma|F_o - F_c|/\Sigma F_o$; 5% of the data that were excluded from refinement were used in the R_{free} calculation.   §The root mean square deviation from ideality for bond angle and length is presented.

Fig. 2. Views of the Kv1.2–β₂ subunit complex. (**A**) Stereoview of a ribbon representation from the side, with the extracellular solution above and the intracellular solution below. Four subunits of the channel (including the T1 domain, voltage sensor, and pore) are colored uniquely. Each subunit of the β subunit tetramer is colored according to the channel subunit it contacts. The NADP⁺ cofactor bound to each β subunit is drawn as black sticks. TM indicates the integral membrane component of the complex. (**B**) Stereoview of a single subunit of the channel and β subunit viewed from the side. Labels correspond to transmembrane helices (S1 to S6); the Pro-Val-Pro sequence in S6 (PVP); and the N (N) and C (C) termini of the Kv1.2 and β subunits. The position of the N terminus of the β subunit, which is located on the side furthest away from the viewer, is indicated by an arrow. (**C**) Stereoview of a ribbon representation viewed from the extracellular side of the pore. Four subunits are colored uniquely. The figure was generated with Ribbons (53).

The α helices of the ion conduction pore (S5, pore helix, and S6) (Fig. 2B) relate to the α helices of the voltage sensor in an unexpected manner. The voltage sensor is latched around the pore of an adjacent subunit. This is most easily appreciated by viewing the channel along its fourfold axis from outside the cell and noting the manner in which the pore and voltage-sensor units engage each other around the tetramer (Fig. 2C). The connection between the pore and the voltage sensor of a given subunit is made by the S4-S5 linker helix, which runs parallel to the intracellular membrane surface just at the level of the inner-helix bundle crossing (Fig. 2, A and B). The inner-helix bundle was defined in the KcsA (a non–voltage-dependent K⁺ channel) channel as the right-handed bundle of four inner helices (one from each subunit, S6 in Kv1.2) that line the pore on the intracellular side of the selectivity filter (Fig. 3, A and B) (4). This

bundle structure is important because it forms an expandable constriction (the bundle crossing) for opening and closing the ion-conduction pore, known as the activation gate.

In the Kv1.2-β2 crystal structure, the voltage-sensor helices are somewhat tilted in the membrane, but they have a native-like transmembrane orientation with hydrophilic loops between helices at the membrane surfaces. In the accompanying Research Article (35), which is focused on voltage-dependent gating, we outline the evidence that the connections between the voltage sensors and pore have maintained a native configuration.

The ion conduction pore. The structures of four different prokaryotic K+ channels have been determined by x-ray crystallography, including KcsA (4, 36), MthK (37) (a Ca2+-gated K+ channel), KirBac (38) (an inward-rectifier K+ channel), and KvAP (30) (a voltage-dependent K+ channel). A comparison of these channel structures emphasizes two

important aspects of K+ channels: (i) the structure of the K+ selectivity filter on the extracellular side of the pore is highly conserved; and (ii) the inner pore (between the selectivity filter and intracellular solution) varies in its conformation. Structural conservation of the selectivity filter underlies the conserved mechanism of selective ion conduction in K+ channels, whereas variation of the inner pore structure is related to conformational changes that open and close the pore. In the published structures, KcsA and KirBac appear to be closed on the basis of the dimensions of the pore at the narrowest point of the inner-helix bundle (Fig. 3, A and B, the bundle crossing), whereas MthK and KvAP appear to be open. In Fig. 3, A and B, two subunits of the Kv1.2 pore (red) have been superimposed on KcsA (closed, gray) and KvAP (opened, blue) (KvAP inner helices are in a similar position to MthK inner helices). The inner helices of Kv1.2 are in between KcsA and KvAP but much closer

to KvAP at the inner-helix bundle crossing. The pore of Kv1.2 has a diameter of about 12 Å at the bundle crossing, suggesting that the pore in the crystal structure is open.

The superposition of pores in Fig. 3 provides a vivid picture of the large inner-helical motions that must occur when a K+ channel opens. Functional studies in *Shaker* K+ channels are consistent with this picture (39, 40). The accessibility of site-directed cysteine residues introduced into the inner helices points to the bundle crossing as the functional constriction for closure. Positions "below" the bundle crossing react with sulfhydryl reagents added to the intracellular side of the membrane whether or not the channel is open, but positions "above" the bundle crossing require the channel to open (40). A tight constriction prevents even Ag+ ions from passing the bundle crossing when the *Shaker* K+ channel's pore is closed, but after it opens, large organic quaternary ammonium cations and hydrophobic polypeptides can enter into the inner pore and plug Kv channels (15, 16, 41, 42).

The inner helices of Kv1.2 contain the amino acid sequence Pro-Val-Pro, which is highly conserved among *Shaker* family Kv channels. These amino acids curve the S6 inner helices so that they run almost parallel to the membrane near the intracellular surface (Fig. 2B and Fig. 3, A and B). Curved inner helices appear to be a specialized adaptation for Kv channels, not *Shaker* channels per se. In KvAP, a prokaryotic Kv channel, a Gly residue produces a similar curvature of the inner helices (Fig. 3, A and B). Thus, the sequence Pro-X-Pro is one way to produce the curve and glycine is another. Both achieve the same structural requirement. In (35), we show why a curved inner helix is required for coupling the voltage sensor to the pore in Kv channels.

The α-helical linkers connecting the T1 domain to S1 project in a radial direction outward from the channel's central axis to create a wide space between the T1 domain and the pore (Fig. 2A). This would seem to accomplish two functions: It would allow the inner helices to undergo their large gating movements to open the pore without interference from the T1 domain or linkers, and it would provide low-resistance diffusion pathways between the pore entryway and the cytoplasm. A surface rendering of Kv1.2 shows one of these diffusion pathways, termed a side portal, above the T1 domain (Fig. 4A). Four side portals each have a diameter of 15 to 20 Å. The electrostatic potential of this region will attract cations owing to the presence of multiple negatively charged amino acids on the surface (Fig. 4A, red), particularly on the rim of the side portals. This feature of the channel is reminiscent of the intracellular entryway to the acetylcholine receptor ion channel (43).

The dimensions and electrostatic properties of the side portals provide information on an
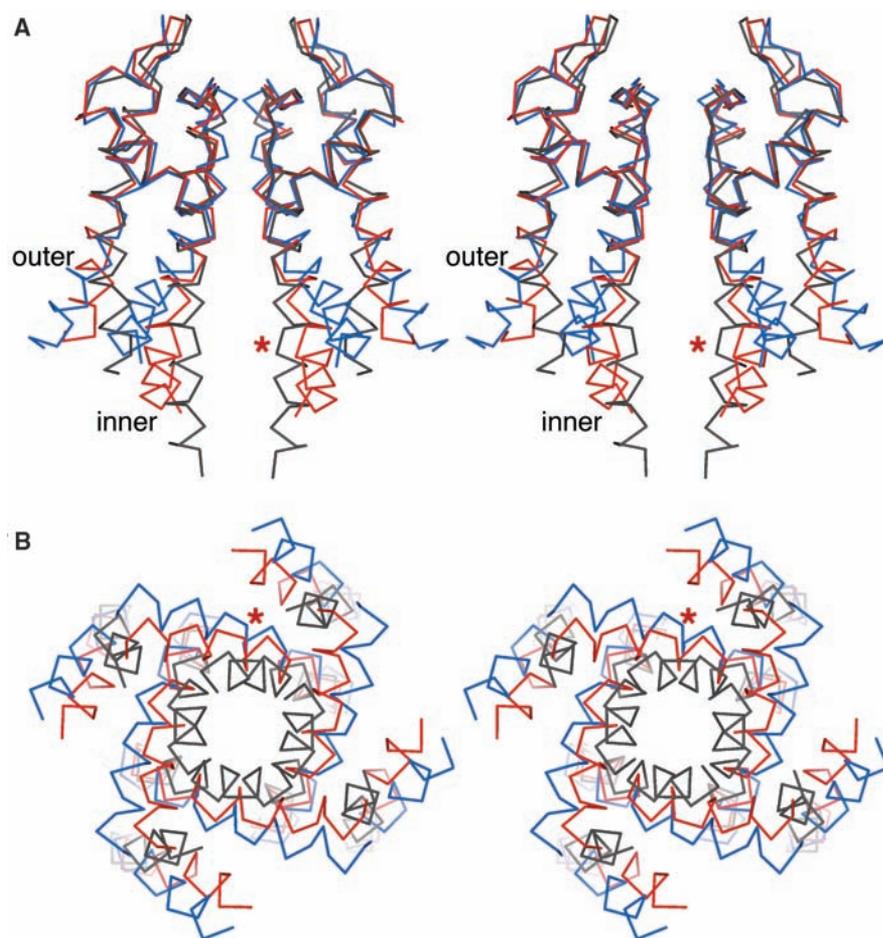
Fig. 3. Comparison of the pore of three K+ channels. Stereoviews of the Kv1.2 K+ channel (red, residues 325 to 418), the KcsA K+ channel (gray, PDB ID 1K4C, residues 26 to 119), and the KvAP K+ channel (blue, PDB ID 1ORQ, residues 147 to 240) are shown in (**A**), with two subunits viewed from the side and in (**B**), with four subunits viewed along the pore axis from the intracellular solution. Channels were superimposed by aligning main-chain atoms of the selectivity filter and pore helices. Outer and inner helices refer to S5 and S6 in Kv1.2. The inner helices form the bundle crossing at the narrowest point, as shown in (B). An asterisk indicates the position of the Pro-Val-Pro sequence on the inner (S6) helix of Kv1.2 and also corresponds to the position of Gly 229 in KvAP. The figure was generated with Molscript (54).

important form of gating known as N-type or "ball and chain" inactivation that occurs in a subset of *Shaker* family Kv channels (*15, 16*). After membrane depolarization, this subset produces transient K⁺ currents called "A currents," rather than sustained "delayed rectifier" K⁺ currents (*1*). A-current channels and delayed-rectifier channels confer different electrical behaviors on cells. For example, delayed-rectifier channels such as Kv1.2 return the membrane potential promptly to its resting value after an action potential, whereas A-current channels allow certain neurons to fire action potentials at a frequency proportional to the total synaptic input current from other neurons (*44*). From a structural perspective, the distinction between A-current channels and delayed rectifiers is subtle: A-current channels have just the right composition of amino acids on their intracellular N terminus—or on the N terminus of an associated β subunit—to allow the terminus itself to enter the inner pore and plug (inactivate) the Kv channel after it opens its activation gate (*15, 16, 32*). This kind of N terminus, called an inactivation gate or inactivation peptide, makes an A-current Kv channel transient. Upon membrane depolarization, the pore opens and conducts K⁺ ions, but shortly thereafter it becomes inactivated, as demonstrated by Aldrich and colleagues (*15, 16*). These authors also defined the amino acids necessary for the N terminus to inactivate the pore of a *Shaker* family Kv channel (*45, 46*). The first ~10 amino acids should be predominantly hydrophobic, followed by a sequence of hydrophilic and positively charged amino acids. They concluded that the hydrophobic stretch becomes buried in a hydrophobic environment and that the hydrophilic region is important for long-range electrostatic interactions between the inactivation gate and pore. Further studies using the mammalian homolog of *Shaker*, Kv1.4, led to the proposal that the hydrophobic region of the N terminus (of a β subunit inactivation peptide) reaches into the inner pore, which is lined by hydrophobic amino acids, and that positively charged amino acids from the hydrophilic region make electrostatic interactions with negatively charged amino acids from the T1 domain and linkers to S1 (*12, 47*). We can now see in the Kv1.2 structure that the corresponding negatively charged amino acids reside on the surface of the side portals (Fig. 4A, asterisk). It is easy to imagine an inactivation peptide in an A-current Kv channel snaking through a side portal with its positive amino acids lying against the negative surface and its hydrophobic amino acids extending to the inner pore (Fig. 4B).

Relationship between the pore, T1 domain, and β subunit catalytic site. The first and, to date, the only firmly established role of β subunits of *Shaker* Kv channels is to confer inactivation (*32, 48*). The β₁ subunit has on its N terminus an amino acid sequence that

has the chemical requirements described above for an inactivation peptide. Thus, when β₁ is coexpressed with a *Shaker* Kv channel, it produces N-type inactivation (*32*). The N terminus of the structured region of the β₂ subunit in the Kv1.2-β₂ complex is located roughly 80 Å from the pore, whereas the N terminus of the structured region of the channel (T1) is about 50 Å from the pore (Fig. 2B). *Shaker* Kv channels that possess N-type inactivation peptides have at least 30 additional amino acids preceding the T1 domain, and the β₁ subunit has approximately 70 additional amino acids on

its N terminus. As extended polypeptide chains, these N termini are easily long enough to reach the pore to produce N-type inactivation.

The β subunits probably have other functions besides inactivation, because not all β subunits have an N terminal inactivation peptide. For example, the β₂ subunit used to produce the Kv1.2-β2 crystals, although nearly identical to β₁ through the structured region of β₂ (amino acid 36 to 361), does not have an N terminal inactivation sequence and does not produce inactivation when associated with Kv channels in membranes (*48, 49*). The β subunits must
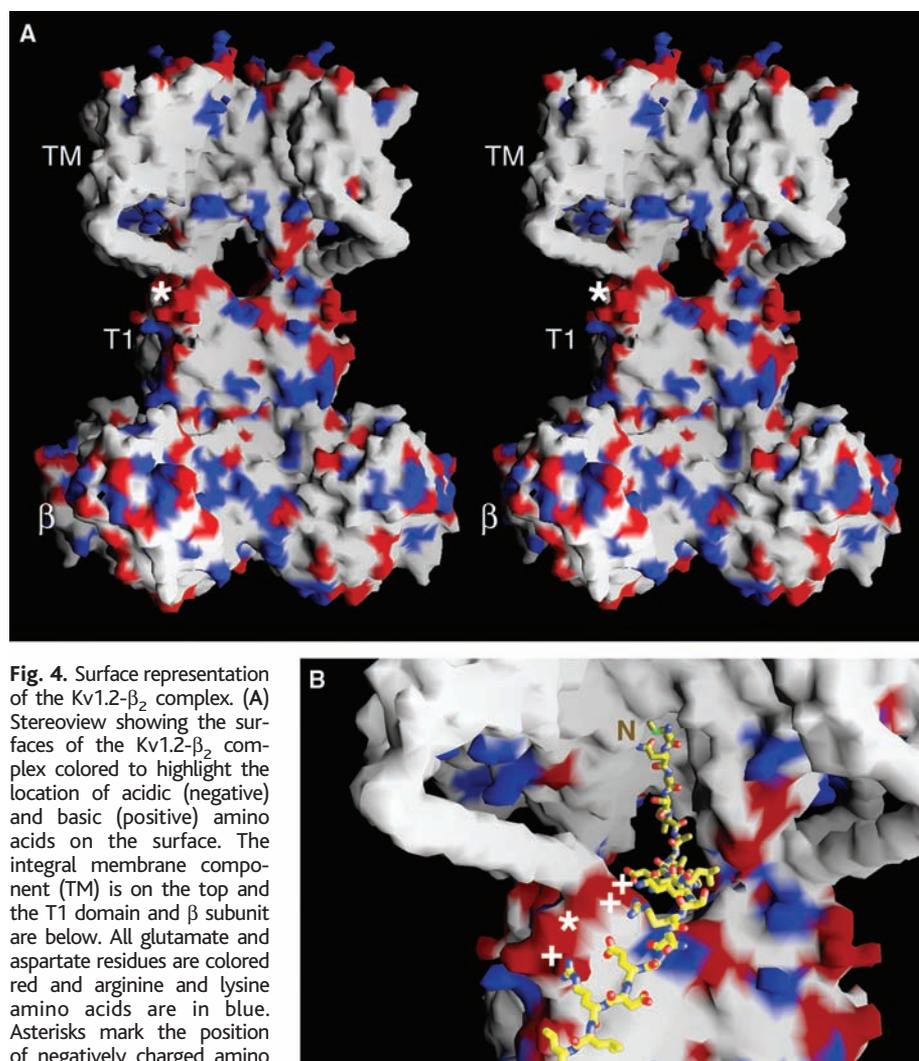
Fig. 4. Surface representation of the Kv1.2-β₂ complex. (**A**) Stereoview showing the surfaces of the Kv1.2-β₂ complex colored to highlight the location of acidic (negative) and basic (positive) amino acids on the surface. The integral membrane component (TM) is on the top and the T1 domain and β subunit are below. All glutamate and aspartate residues are colored red and arginine and lysine amino acids are in blue. Asterisks mark the position of negatively charged amino acids Glu¹²⁸, Asp¹²⁹, and Glu¹³⁰ on T1, which, in the Kv1.4 K⁺ channel, interact with positively charged amino acids on inactivation peptides (*47*). The large holes (side portals) above the T1 domain and below the integral membrane channel are passages connecting the cytoplasm to the pore. (**B**) Hypothetical model for the binding of an inactivation peptide to the channel. A portion of the surface of the T1 and integral membrane components of the complex is shown in the same orientation and colored as in (A). An inactivation peptide corresponding to the 22 N-terminal residues of β₁ has been modeled in an extended conformation to enter a side portal and plug the inner pore of the channel. Three positive residues (+) located at positions 13, 15, and 20 from the N terminus were placed at the site of interaction with the negatively charged patch of residues on T1 [asterisk (*12*)], whereas the hydrophobic residues at the N terminus were placed at the inner pore where they are known to bind and block the flow of potassium (*47*). To show entry of the peptide's N terminus into the inner pore in this figure, the following portions of the channel subunit closest to the viewer were removed: residues 312 to 329 (S4-S5 linker and part of S5) and residues 405 to 421 (the C-terminal end of S6.) The figure was generated with GRASP software (*55*).

have additional functions. The observation that β subunits can influence levels of channel expression has led to one hypothesis that they may function as chaperones for the channel (*50*, *51*). The presence of conserved catalytic residues for hydride transfer in the enzyme active site of β subunits forms the basis of another hypothesis, that β subunits are important for a catalytic function (*22–24*). The Kv channel could regulate the activity of the β subunit, or perhaps more likely, the β subunit could regulate the activity of the channel. A β subunit "redox sensor" would allow direct coupling of membrane electrical activity to the redox state of a cell.
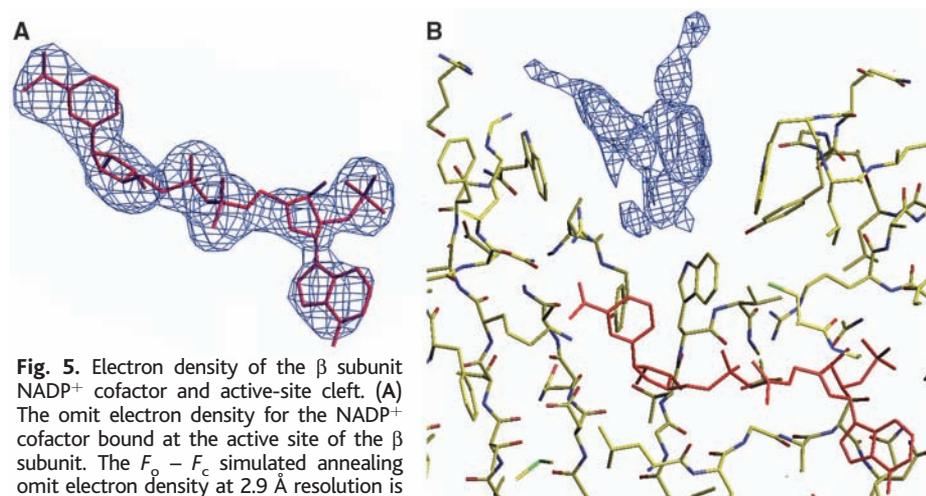
The active site of β subunits has an NADP$^+$ cofactor and catalytic residues for hydride transfer. This cofactor is present in the Kv1.2-β2 crystal structure (Fig. 5A). In addition, there is poorly defined extra density overlying the active site in all of our electron density maps (Fig. 5B). The surface of the active-site cleft, where this material is bound, is quite hydrophobic and has many aromatic amino acids (Fig. 5B). The density is probably either from a polypeptide chain or from a large organic molecule. If it represents a polypeptide chain, it could either be part of the channel or it could be co-isolated with the channel during purification. The channel in the crystal structure contains 31 disordered amino acids on its N terminus (N terminal to T1) and 78 on its C terminus. Binding either the N terminus or the C terminus near the β subunit active site, with an affinity that depends on whether the cofactor is oxidized or reduced, could affect Kv channel function. For example, in some *Shaker* family Kv channels, binding of the polypeptide chain preceding T1 could affect the availability of the inactivation gate. The C-terminal polypeptide could potentially influence gating because it is connected directly to the inner helices, which must undergo large movements to gate the pore open and closed. The Kv1.2-β2 crystal structure should help in the design of experiments to test these ideas.

Summary. This work describes the crystal structure of the mammalian *Shaker* family Kv channel Kv1.2 in complex with the β$_2$ subunit. Both proteins were coexpressed in *Pichia pastoris*. Two critical factors were essential for obtaining crystals and determining the structure. A mixture of lipids and detergent was used throughout purification and crystallization, and many steps were taken to minimize oxidation. The importance of lipids in this project may suggest the general application of lipids in membrane protein structural studies in the future. The *I*4 crystal lattice of alternating "membrane" and water layers comes very close to a native arrangement for the channel. The relationships between the integral membrane components, the intracellular T1 domain, and the β subunit bound to the T1 domain are consistent with electrophysiological studies of the inactivation process in *Shaker* K$^+$ channels. The pore of Kv1.2 is similar in structure to that of prokaryotic K$^+$ channels. Curved inner helices are produced by the sequence Pro-X-Pro in *Shaker* family K$^+$ channels and by Gly in KvAP and probably many other Kv channels. The Kv1.2 pore is in an open conformation. Large side portals between the T1 domain and the pore connect the pore to the cytoplasm. Electrostatic properties of the side portals are consistent with long-range electrostatic steering of inactivation peptides. An NADP$^+$ cofactor, catalytic residues, and extra density at the β subunit active-site cleft suggest experiments for testing the influence of β subunit catalytic function on K$^+$ channel activity. The voltage sensors are in the "membrane" layer of the crystal and appear to be unperturbed.

Fig. 5. Electron density of the β subunit NADP$^+$ cofactor and active-site cleft. (**A**) The omit electron density for the NADP$^+$ cofactor bound at the active site of the β subunit. The $F_o - F_c$ simulated annealing omit electron density at 2.9 Å resolution is contoured at 4σ (blue mesh) and shown with the NADP$^+$ molecule drawn as red sticks. (**B**) "Extra" density in the active-site cleft of the β subunit. A 2$F_o - F_c$ electron density map to 2.9 Å resolution and contoured at 0.8σ is drawn in a pocket above the catalytic residues. The NADP$^+$ cofactor is shown as red sticks.

References and Notes

1. B. Hille, *Ion Channels of Excitable Membranes* (Sinauer Associates, Sunderland, MA, ed. 3, 2001).
2. G. Yellen, *Q. Rev. Biophys.* **31**, 239 (1998).
3. R. MacKinnon, *Angew. Chem. Int. Ed. Engl.* **43**, 4265 (2004).
4. D. A. Doyle *et al.*, *Science* **280**, 69 (1998).
5. D. H. Hackos, T. H. Chang, K. J. Swartz, *J. Gen. Physiol.* **119**, 521 (2002).
6. Z. Lu, A. M. Klem, Y. Ramu, *J. Gen. Physiol.* **120**, 663 (2002).
7. S. M. Webster, D. del Camino, J. P. Dekker, G. Yellen, *Nature* **428**, 864 (2004).
8. B. L. Tempel, D. M. Papazian, T. L. Schwarz, L. Y. Jan, Y. N. Jan, *Science* **237**, 770 (1987).
9. A. Kamb, L. E. Iverson, M. A. Tanouye, *Cell* **50**, 405 (1987).
10. O. Pongs *et al.*, *EMBO J.* **7**, 1087 (1988).
11. A. Kreusch, P. J. Pfaffinger, C. F. Stevens, S. Choe, *Nature* **392**, 945 (1998).
12. J. M. Gulbis, M. Zhou, S. Mann, R. MacKinnon, *Science* **289**, 123 (2000).
13. O. Sokolova, L. Kolmakova-Partensky, N. Grigorieff, *Structure* (*Camb.*) **9**, 215 (2001).
14. W. R. Kobertz, C. Williams, C. Miller, *Biochemistry* **39**, 10347 (2000).
15. T. Hoshi, W. N. Zagotta, R. W. Aldrich, *Science* **250**, 533 (1990).
16. W. N. Zagotta, T. Hoshi, R. W. Aldrich, *Science* **250**, 568 (1990).
17. S. Sewing, J. Roeper, O. Pongs, *Neuron* **16**, 455 (1996).
18. W. Yu, J. Xu, M. Li, *Neuron* **16**, 441 (1996).
19. H. Rehm, M. Lazdunski, *Proc. Natl. Acad. Sci. U.S.A.* **85**, 4919 (1988).
20. D. N. Parcej, V. E. Scott, J. O. Dolly, *Biochemistry* **31**, 11084 (1992).
21. V. E. Scott *et al.*, *Proc. Natl. Acad. Sci. U.S.A.* **91**, 1637 (1994).
22. T. McCormack, K. McCormack, *Cell* **79**, 1133 (1994).
23. S. W. Chouinard, G. F. Wilson, A. K. Schlimgen, B. Ganetzky, *Proc. Natl. Acad. Sci. U.S.A.* **92**, 6763 (1995).
24. J. M. Gulbis, S. Mann, R. MacKinnon, *Cell* **97**, 943 (1999).
25. K. Nakahira, G. Shi, K. J. Rhodes, J. S. Trimmer, *J. Biol. Chem.* **271**, 7084 (1996).
26. F. J. Sigworth, *Q. Rev. Biophys.* **27**, 1 (1994).
27. F. Bezanilla, *Physiol. Rev.* **80**, 555 (2000).
28. F. Sesti, S. Rajan, R. Gonzalez-Colaso, N. Nikolaeva, S. A. Goldstein, *Nat. Neurosci.* **6**, 353 (2003).
29. V. Ruta, Y. Jiang, A. Lee, J. Chen, R. MacKinnon, *Nature* **422**, 180 (2003).
30. Y. Jiang *et al.*, *Nature* **423**, 33 (2003).
31. W. Stuhmer *et al.*, *EMBO J.* **8**, 3235 (1989).
32. J. Rettig *et al.*, *Nature* **369**, 289 (1994).
33. D. N. Parcej, L. Eckhardt-Strelau, *J. Mol. Biol.* **333**, 103 (2003).
34. Materials and methods are available as supporting material on *Science* Online.
35. S. B. Long, E. B. Campbell, R. MacKinnon, *Science* **309**, 903 (2005); published online 7 July 2005 (10.1126/science.1116270).
36. Y. Zhou, J. H. Morais-Cabral, A. Kaufman, R. MacKinnon, *Nature* **414**, 43 (2001).
37. Y. Jiang *et al.*, *Nature* **417**, 515 (2002).
38. A. Kuo *et al.*, *Science* **300**, 1922 (2003).
39. D. del Camino, M. Holmgren, Y. Liu, G. Yellen, *Nature* **403**, 321 (2000).
40. Y. Liu, M. Holmgren, M. E. Jurman, G. Yellen, *Neuron* **19**, 175 (1997).
41. D. del Camino, G. Yellen, *Neuron* **32**, 649 (2001).
42. C. M. Armstrong, *J. Gen. Physiol.* **58**, 413 (1971).
43. A. Miyazawa, Y. Fujiyoshi, M. Stowell, N. Unwin, *J. Mol. Biol.* **288**, 765 (1999).
44. J. A. Connor, C. F. Stevens, *J. Physiol.* **213**, 1 (1971).
45. R. D. Murrell-Langnado, R. W. Aldrich, *J. Gen. Physiol.* **102**, 949 (1993).
46. R. D. Murrell-Langnado, R. W. Aldrich, *J. Gen. Physiol.* **102**, 977 (1993).
47. M. Zhou, J. H. Morais-Cabral, S. Mann, R. MacKinnon, *Nature* **411**, 657 (2001).
48. S. H. Heinemann, J. Rettig, H. R. Graack, O. Pongs, *J. Physiol.* **493**, 625 (1996).

49. K. McCormack, T. McCormack, M. Tanouye, B. Rudy, W. Stuhmer, *FEBS Lett.* **370**, 32 (1995).
50. G. Shi *et al.*, *Neuron* **16**, 843 (1996).
51. N. Nagaya, D. M. Papazian, *J. Biol. Chem.* **272**, 3022 (1997).
52. T. A. Jones, J. Y. Zou, S. W. Cowan, M. Kjeldgaard, *Acta Crystallogr.* **A47**, 110 (1991).
53. M. Carson, *Methods Enzymol.* **277**, 493 (1997).
54. P. Kraulis, *J. Appl. Crystallogr.* **24**, 946 (1991).
55. A. Nicholls, K. A. Sharp, B. Honig, *Proteins* **11**, 281 (1991).
56. We thank A. Lee, V. Ruta, and members of the MacKinnon

Voltage Sensor of Kv1.2: Structural Basis of Electromechanical Coupling

Stephen B. Long, Ernest B. Campbell, Roderick MacKinnon*

Voltage-dependent ion channels contain voltage sensors that allow them to switch between nonconductive and conductive states over the narrow range of a few hundredths of a volt. We investigated the mechanism by which these channels sense cell membrane voltage by determining the x-ray crystal structure of a mammalian *Shaker* family potassium ion (K+) channel. The voltage-dependent K+ channel Kv1.2 grew three-dimensional crystals, with an internal arrangement that left the voltage sensors in an apparently native conformation, allowing us to reach three important conclusions. First, the voltage sensors are essentially independent domains inside the membrane. Second, they perform mechanical work on the pore through the S4-S5 linker helices, which are positioned to constrict or dilate the S6 inner helices of the pore. Third, in the open conformation, two of the four conserved Arg residues on S4 are on a lipid-facing surface and two are buried in the voltage sensor. The structure offers a simple picture of how membrane voltage influences the open probability of the channel.

Voltage-dependent ion channels open in response to changes in voltage across the cell membrane (*1*). In this process, the membrane electric field performs mechanical work to alter the channel's conformation within the membrane. The work arises from the force exerted by the electric field on charged amino acids, termed gating charges (*1–3*). The size of the gating charge is very large (*4*), accounting for the exquisite sensitivity of voltage-dependent ion channels to small changes in membrane voltage. To understand this process, one must first answer two questions: How do gating charges move within the membrane electric field? And how are these movements mechanically coupled to opening and closing of the pore?

No experimentally based model has yet provided answers to both of these questions. So far, little progress has been made toward the second question concerning the mechanical coupling of voltage-sensor movements to the pore. Most effort has focused on how the gating charges move; the main subject of study has been the *Shaker* voltage-dependent K+ (Kv) channel, and numerous models have been put forth. One fundamental constraint for any model is that when a *Shaker* K+ channel opens, it transfers the net equivalent of 12 to 14 positive elementary charges across the membrane electric field from inside to outside, and most of this charge is carried by four S4 Arg residues on each of four identical channel subunits (*4–6*).

A guiding assumption underlying most models for the voltage sensor has been that the S4 helix with its Arg residues is completely (*7–10*), or mostly (*11*), sequestered from the membrane, in order to protect the charges from the lipid's low dielectric environment. To accomplish this, most models postulate that the S4 helix inserts into a groove at the interface between adjacent subunits of the K+ channel tetramer, such that pore α helices S5 and S6 form a wall on one side of S4 and voltage-sensor α helices S1 to S3 form a wall on the other side, the lipid-facing perimeter, to create a gating channel or protein-lined canaliculus for S4 (*7–10, 12*). This arrangement would allow the S4 helix to move its charged amino acids across the membrane without exposing them to the lipid environment.

How and to what extent S4 moves has been the subject of much debate. Gating-dependent reactivity of sulfhydryl reagents with cysteine residues led to an initial hypothesis of large (~15 Å) translations of S4 in some models (*13–17*). But very small distance changes measured in fluorescence resonance energy transfer (FRET) experiments suggested much smaller movements of S4 across the membrane (*18, 19*). Crevices surrounding S4 were invoked to account for the sulfhydryl reactivity in the setting of these smaller movements, with translations and/or rotations of S4 occurring across a narrow neck inside an hourglass-shaped canaliculus. In the transporter model hypothesis, the S4 does not change its depth in the membrane at all (less than 3 Å movement) (*18, 20*). Instead, the field is moved over the S4 charges by alternately opening and closing crevices to the internal and external solutions.

The above models of voltage-dependent gating vary in detail, but they have had two essential features in common. First, the S4 helix is sequestered from the lipid membrane [although Larsson and colleagues proposed that a surface of S4 could be exposed to lipid (*11*)]. Second, the voltage-sensor helices S1 to S4 are packed tightly against the α helices of the pore. In other words, it was reasonably assumed that voltage-dependent ion channels are like conventional α-helical membrane proteins that form a fairly rigid disk of helices in the membrane. A first hint that a rigid disk of helices might not pertain to voltage-dependent ion channels came from the demonstration that the voltage sensor (S1 to S4) from the *Shaker* Kv channel could be spliced onto the pore of KcsA (a non–voltage-dependent K+ channel) to confer voltage-dependent gating (*21*). This finding implied that the voltage sensor might be an almost-independent domain, because if it had to form a large interface through helix packing with the pore, the chimera would likely not function.

The first atomic structures of a prokaryotic Kv channel (KvAP) also implied that the voltage sensors are loosely attached to the pore (*22*). One of these [Protein Data Bank (PDB) ID 1ORS] was of an isolated voltage-sensor domain, which surprisingly could be expressed in the membrane by itself (without the pore). Another, which is a full-length channel structure (PDB ID 1ORQ), showed the voltage-

Howard Hughes Medical Institute, Laboratory of Molecular Neurobiology and Biophysics, Rockefeller University, 1230 York Avenue, New York, NY 10021, USA.

*To whom correspondence should be addressed. E-mail: mackinn@rockefeller.edu